Free Vibration Analysis of Arbitrarily Shaped Plates With Smoothly Varying Free Edges Using NDIF Method

S. W. Kang[1]
Department of Mechanical Systems Engineering,
Hansung University,
389, 2-ga, Samsun-dong, Sungbuk-gu,
Seoul 136-792, Korea
e-mail: swkang@hansung.ac.kr

I. S. Kim

J. M. Lee

School of Mechanical and Aerospace
Engineering,
Seoul National University,
San 56-1 Shinlim-dong, Kwanak-gu,
Seoul 151-742, Korea

The so-called non-dimensional influence function method that was developed by the authors is extended to free vibration analysis of arbitrarily shaped plates with the free boundary condition. A method proposed in this paper can be applied to plates with only smoothly varying boundary shapes. In the proposed method, a local polar coordinate system has been employed at each boundary node to effectively consider the free boundary condition, which is much more complex than the simply supported or clamped boundary condition. The local coordinates system devised allowed us to successfully deal with the radius of curvature involved in the free boundary condition, and, as a result, the accuracy of the proposed method has been reinforced. Finally, verification examples showed that the natural frequency and mode shapes obtained by the proposed method agree excellently with those given by other analytical or numerical methods.
[DOI: 10.1115/1.2730531]

Keywords: NDIF method, arbitrarily shaped plate, free vibration, non-dimensional dynamic influence function

1 Introduction

The so-called non-dimensional influence function (NDIF) method (a method using non-dimensional dynamic influence functions) [1–5] that was introduced by the authors has advantages in solving free vibration problems, compared with the finite element method (FEM) [6] and the boundary element method [7,8]. Since no interpolation function is used in the NDIF method (two basis functions are used instead), no integration procedure is involved in its theoretical formulation. As a result, the NDIF method needs a small amount of numerical calculation and yields rapidly converged results (natural frequencies and mode shapes). However, the NDIF method has the weak points that it needs an additional treatment to remove spurious eigenvalues [4], it cannot be directly applied to a multi-connected domain problem and the multi-domain method should be used [3], and it may have an ill-conditioned system matrix when too many nodes are used.

In this paper, the NDIF method is extended to the free vibration analysis of *free* plates of smooth, arbitrary shapes having no corner. Polygonal plates having corners, such as triangular and rectangular ones, will be considered in another paper, because two cases with and without corners are quite different in their theoretical formulations.

As surveyed in the previous paper [5] reported by the authors, many researchers have studied the free vibrations of plates with a variety of shapes and boundary conditions [9–25]. Recently, the Trefftz method and the method of fundamental solutions similar to the NDIF method have been introduced [26–29]. However, analytical methods for arbitrarily shaped plates with the free boundary condition have been little reported in the open literature to the authors' best knowledge. This rarity may result from the fact that the free boundary condition has many mathematical difficulties because it consists of two complicated differential equations of higher order. In this paper (to settle the aforementioned difficulties), a local polar coordinate system is devised to simplify the free boundary condition that is generally expressed by the normal-tangential coordinate system [30]. A detailed explanation on the local polar coordinate system will be given in the body of the paper.

On the other hand, similar to previous papers [4,5] dealing with clamped or simply supported boundary condition, the linear superposition of non-dimensional dynamic influence functions is assumed as an approximate solution for the flexural vibration of free plates in the paper. By using the local polar coordinates system, the free boundary condition is applied to the approximate solution. One can then obtain the system matrix, the singular values of which consist of correct eigenvalues and spurious ones. On the other hand, the spurious eigenvalues are removed by using a method similar to that used in the previous paper [4].

Unlike the previous papers [4,5], it should be noted in this paper dealing with the free boundary condition that a functional value of the non-dimensional dynamic influence function diverges when the distance between two nodes involved in the function becomes zero. In this paper, this divergence problem is successfully overcome by extracting the limit form of the non-dimensional dynamic influence function.

In addition, an approach similar to that used in the previous work [4,5] is used to remove spurious eigenvalues, which correspond to the eigenvalues of a membrane with the same shape as the free plate of interest. The validity and accuracy of eigenvalues and mode shapes found by the proposed method were verified by several comparison tests.

2 Theoretical Development

2.1 Governing Equation and Boundary Conditions for Free Plates. Consider a thin, isotropic plate of which the boundary Γ is depicted with the dotted line in Fig. 1. The governing differential equation for free flexural vibration of this plate has the form [30]

[1]Corresponding author.

Contributed by the Technical Committee on Vibration and Sound of ASME for publication in the JOURNAL OF VIBRATION AND ACOUSTICS. Manuscript received February 19, 2006; final manuscript received November 8, 2006; published online July 14, 2008. Assoc. Editor Jonathan A. Wickert.

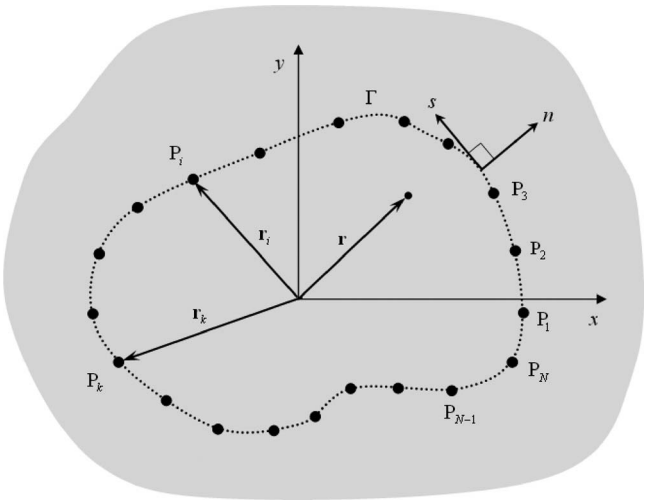

Fig. 1 An arbitrarily shaped plate depicted by the dotted contour along which *N* boundary nodes are distributed

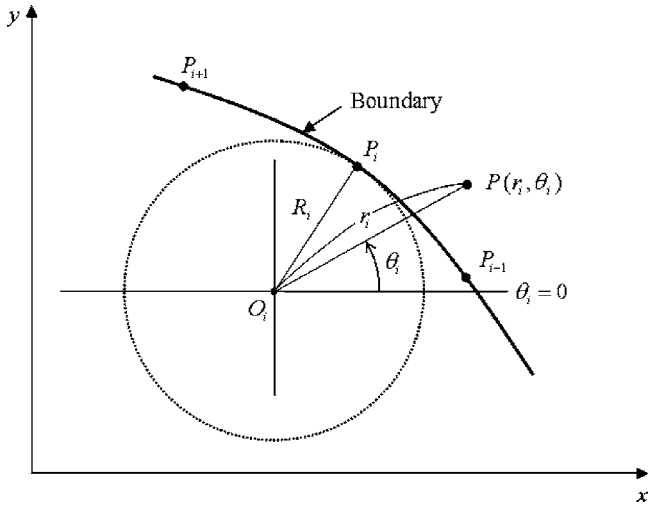

Fig. 2 Local polar coordinates system (r_i, θ_i) for considering the free boundary condition of node P_i (the origin O_i of the coordinates system is located at the center of curvature measured at node P_i, and R_i is the radius of curvature measured at node P_i)

$$D\nabla^4 w + \rho_s \frac{\partial^2 w}{\partial t^2} = 0 \tag{1}$$

where the operator $\nabla^4 = \nabla^2\nabla^2$ is known as the biharmonic operator, $w = w(\mathbf{r}, t)$is the transverse deflection at position vector $\mathbf{r}$, ρ_s is the surface density of the plate, and $D = Eh^3/12(1-\nu^2)$ is the flexural rigidity. If the plate vibration is assumed as a harmonic vibration $w(\mathbf{r}, t) = W(\mathbf{r})f(t)$, where $W(\mathbf{r})$ depends on the spatial coordinate only and $f(t)$ is a time-dependent harmonic function of circular frequency ω, Eq. (1) leads to

$$\nabla^4 W - \Lambda^4 W = 0 \tag{2}$$

where $\Lambda = (\rho_s \omega^2 / D)^{1/4}$ is the frequency parameter. Furthermore, if the boundary of the plate is assumed as a free edge, the boundary conditions are

$$M_n[W(\mathbf{r})] = 0 \tag{3}$$

$$V_n[W(\mathbf{r})] = 0 \quad \text{on } \Gamma \tag{4}$$

where M_n and V_n denote the bending moment and vertical force at the edge, respectively [30]. For the particular case of a circular plate [30], M_n and V_n can be expressed in the polar coordinates system (r, θ), respectively, as follows

$$M_r = -D\left(\frac{\partial^2 W}{\partial r^2} + \frac{\nu}{r}\frac{\partial W}{\partial r} + \frac{\nu}{r^2}\frac{\partial^2 W}{\partial \theta^2}\right) \tag{5}$$

$$V_r = -D\left(\frac{\partial^3 W}{\partial r^3} + \frac{1}{r}\frac{\partial^2 W}{\partial r^2} - \frac{1}{r^2}\frac{\partial W}{\partial r} + \frac{2-\nu}{r^2}\frac{\partial^3 W}{\partial r\, \partial \theta^2} - \frac{3-\nu}{r^3}\frac{\partial^2 W}{\partial \theta^2}\right) \tag{6}$$

which will later be referred to for the development of a local polar coordinates system devised in this paper.

2.2 Assumption of the General Solution and Discretization of Boundary Conditions. Similar to the general solution of plates with the clamped boundary condition [4] or the mixed boundary condition [5] in previous research, that of a *free* plate depicted by the dotted line in Fig. 1 is assumed as a linear superposition of the non-dimensional dynamic influence functions defined in an infinite plate

$$W(\mathbf{r}) = \sum_{k=1}^{N} [A_k J_0(\Lambda|\mathbf{r} - \mathbf{r}_k|) + B_k I_0(\Lambda|\mathbf{r} - \mathbf{r}_k|)] \tag{7}$$

where N is the number of nodes distributed along the boundary of the plate, J_0 and I_0 denote Bessel functions of order zero of the first and second kinds, respectively, and $\mathbf{r}_k$ is the position vector for node P_k in Fig. 1. Note that Eq. (7) automatically satisfies the governing equation (2) because it is made by a linear superposition of non-dimensional dynamic influence functions satisfying the governing equation. Because of this fact, an eigensolution of the plate can be obtained by applying the free boundary conditions (3) and (4) to (7).

Since the NDIF method is based on a kind of collocation technique, Eqs. (3) and (4) defined continuously along the boundary Γ are approximated as discrete boundary conditions, which are defined discretely at nodes on Γ

$$M_n[W(\mathbf{r}_i)] = 0 \tag{8}$$

$$V_n[W(\mathbf{r}_i)] = 0 \quad i = 1,2, \ldots, N \tag{9}$$

where $\mathbf{r}_i$ denotes the position vector indicating the ith node on Γ in Fig. 1.

2.3 Introduction of a Local Polar Coordinates System. A polar coordinates system is generally used for plates of only *circular* shape, but in this paper, is used to consider free boundary conditions of an arbitrarily shaped plate with a smoothly varying boundary. For reference, unknown element fields in FE implementations are typically expressed in an element-based local coordinate system. A special idea is devised to express the discrete free boundary conditions (8) and (9) with a polar coordinates system. The idea is to locally define a polar coordinates system for each node as shown in Fig. 2, where the ith local polar coordinates system for node P_i is illustrated.

The key feature of the ith local polar coordinates system is that the normal direction of the boundary measured at node P_i coincides with the radial direction of the coordinates system because the origin (O_i) of the coordinates system is intentionally located at the center of curvature of the boundary measured at node P_i. Because of this feature, Eqs. (8) and (9) can be immediately changed as

$$M_r[W(\mathbf{r}_i)] = 0 \tag{10}$$

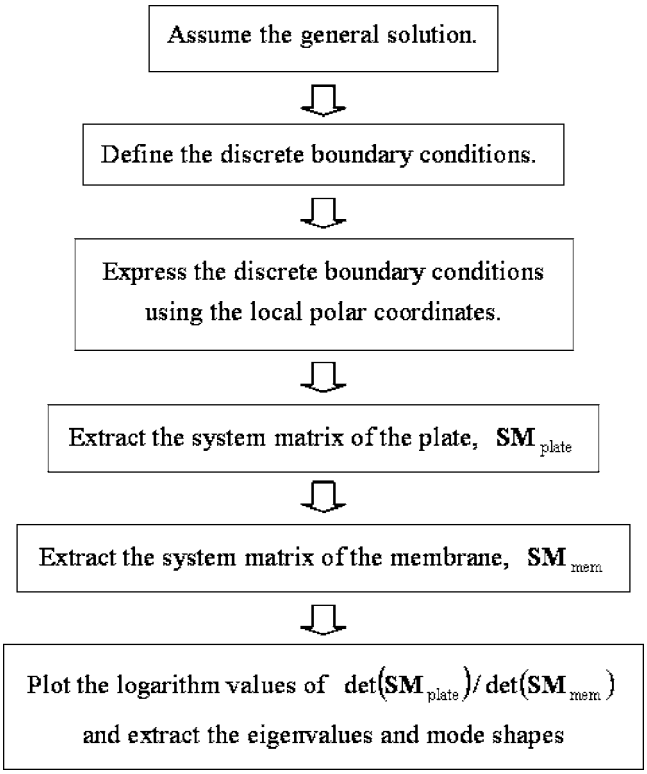

Fig. 3 Flow chart illustrating the theoretical development procedure of the present method

$$V_r[W(\mathbf{r}_i)] = 0 \quad 1,2,\ldots,N \tag{11}$$

which may be explicitly expressed, in the same forms as Eqs. (5) and (6), as follows

$$L_{M(i)}[W(\mathbf{r}_i)] = 0 \tag{12}$$

$$L_{V(i)}[W(\mathbf{r}_i)] = 0 \quad i = 1,2,\ldots,N \tag{13}$$

in which differential operators $L_{M(i)}$ and $L_{V(i)}$ are

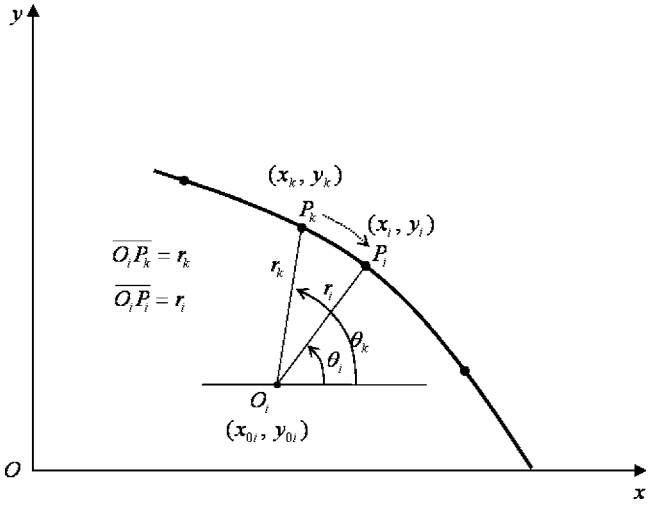

Fig. 4 (x_i, y_i), (x_k, y_k), and (x_{0i}, y_{0i}) denote coordinates of node P_i, node P_k, and origin O_i, respectively, for the global coordinates system (x, y); this figure also illustrates that node P_k approaches node P_i

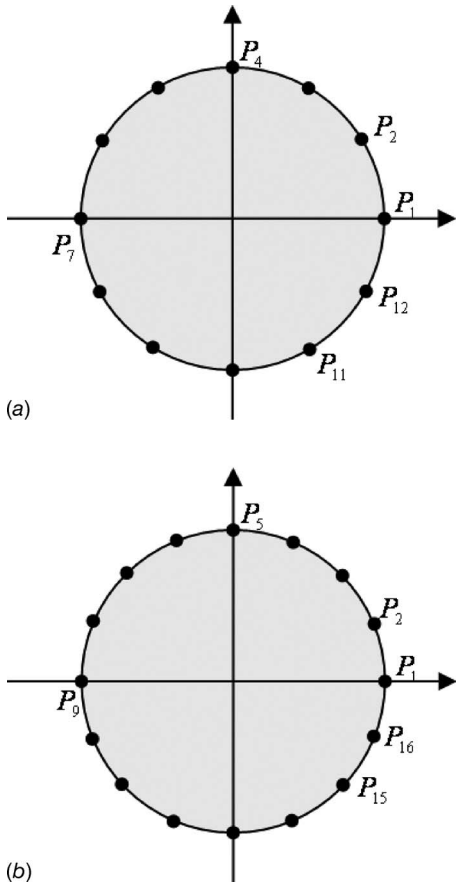

Fig. 5 Discrete boundary nodes of the circular plate when (*a*) *N*=12 and (*b*) *N*=16

$$L_{M(i)} = \frac{\partial^2}{\partial r_i^2} + \frac{\nu}{r_i}\frac{\partial}{\partial r_i} + \frac{\nu}{r_i^2}\frac{\partial^2}{\partial \theta_i^2} \tag{14}$$

$$L_{V(i)} = \frac{\partial^3}{\partial r_i^3} + \frac{1}{r_i}\frac{\partial^2}{\partial r_i^2} - \frac{1}{r_i^2}\frac{\partial}{\partial r_i} + \frac{2-\nu}{r_i^2}\frac{\partial^3}{\partial r_i \partial \theta_i^2} - \frac{3-\nu}{r_i^3}\frac{\partial^2}{\partial \theta_i^2} \tag{15}$$

where r_i and θ_i denote the ith local polar coordinates.

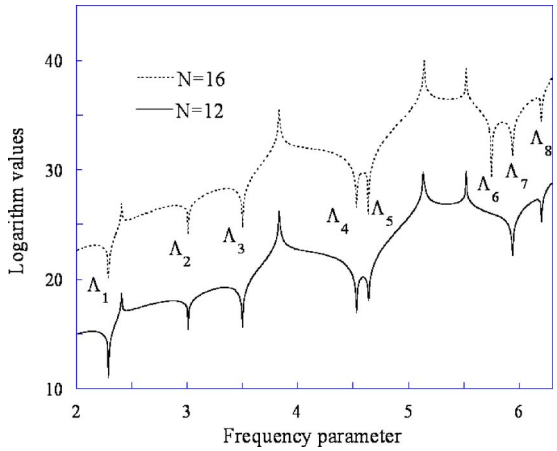

Fig. 6 Logarithm curves for $\det(\mathbf{SM}_{plate})/\det(\mathbf{SM}_{mem})$ of the circular plate when *N*=12 and *N*=16; the resolution of increment of the frequency parameter is 1/1000

Table 1 Eigenvalues of the circular plate obtained by the proposed method, Leissa's source, and FEM

Eigenvalues	Proposed method		Leissa [23]	FEM (ANSYS)		
	$N=12$	$N=16$		4439 nodes	3268 nodes	1937 nodes
CPU time	9.2 min	13 min		2.3 min	1.8 min	1.2 min
Λ_1	2.2939	2.2939	2.2919	2.2969	2.2953	2.2949
Λ_2	3.0115	3.0115	3.0140	3.0159	3.0148	3.0142
Λ_3	3.4991	3.4991	3.4971	3.4990	3.4987	3.4984
Λ_4	4.5291	4.5291	4.5299	4.5357	4.5319	4.5310
Λ_5	4.6393	4.6397	4.6476	4.6380	4.6377	4.6377
Λ_6	None	5.7499	5.7533	5.7464	5.7463	5.7466
Λ_7	5.9365	5.9365	5.9425	5.9425	5.9393	5.9382
Λ_8	6.2054	6.2054	6.2193	6.2193	6.2141	6.2134

2.4 Extraction of the System Matrix. In this section, the system matrix that gives eigenvalues and eigenmodes is extracted by substituting the general solution (7) into the free boundary conditions (12) and (13). Equations (12) and (13) then lead to, respectively

$$L_{M(i)}[W(\mathbf{r}_i)] = \sum_{k=1}^{N} A_k L_{M(i)}[J_0(\Lambda|\mathbf{r}_i - \mathbf{r}_k|)] + \sum_{k=1}^{N} B_k L_{M(i)}[I_0(\Lambda|\mathbf{r}_i - \mathbf{r}_k|)] = 0 \tag{16}$$

$$L_{V(i)}[W(\mathbf{r}_i)] = \sum_{k=1}^{N} A_k L_{V(i)}[J_0(\Lambda|\mathbf{r}_i - \mathbf{r}_k|)] + \sum_{k=1}^{N} B_k L_{V(i)}[I_0(\Lambda|\mathbf{r}_i - \mathbf{r}_k|)] = 0 \tag{17}$$

$$i = 1,2,\ldots,N$$

which may be expressed as a simple matrix equation

$$\mathbf{SM}_{\text{plate}}\mathbf{C} = \mathbf{0} \tag{18}$$

where $2N \times 2N$ system matrix $\mathbf{SM}_{\text{plate}}$ and system vector $\mathbf{C}$ are given by

$$\mathbf{SM}_{\text{plate}} = \begin{bmatrix} \mathbf{SM}_{\text{M}}^{\text{J}} & \mathbf{SM}_{\text{M}}^{\text{I}} \\ \mathbf{SM}_{\text{V}}^{\text{J}} & \mathbf{SM}_{\text{V}}^{\text{I}} \end{bmatrix} \tag{19}$$

$$\mathbf{C} = \{A_1\ A_2 \ldots A_N\ B_1\ B_2 \ldots B_N\}^T \tag{20}$$

and the elements of sub-matrices $\mathbf{SM}_{\text{M}}^{\text{J}}$, $\mathbf{SM}_{\text{M}}^{\text{I}}$, $\mathbf{SM}_{\text{V}}^{\text{J}}$, and $\mathbf{SM}_{\text{V}}^{\text{I}}$ can be calculated by

$$SM_{\text{M}}^{\text{J}}(i,k) = L_{M(i)}[J_0(\Lambda|\mathbf{r}_i - \mathbf{r}_k|)] \tag{21}$$

$$SM_{\text{M}}^{\text{I}}(i,k) = L_{M(i)}[I_0(\Lambda|\mathbf{r}_i - \mathbf{r}_k|)] \tag{22}$$

$$SM_{\text{V}}^{\text{J}}(i,k) = L_{V(i)}[J_0(\Lambda|\mathbf{r}_i - \mathbf{r}_k|)] \tag{23}$$

$$SM_{\text{V}}^{\text{I}}(i,k) = L_{V(i)}[I_0(\Lambda|\mathbf{r}_i - \mathbf{r}_k|)] \tag{24}$$

Finally, in the same approach taken in the authors' previous research [4], the eigenvalues of the free plate can be obtained by plotting logarithm values of $\det(\mathbf{SM}_{\text{plate}})/\det(\mathbf{SM}_{\text{mem}})$, where $\mathbf{SM}_{\text{mem}}$ represents the system matrix of a fixed membrane with the same shape as the free plate. Theoretical development procedures

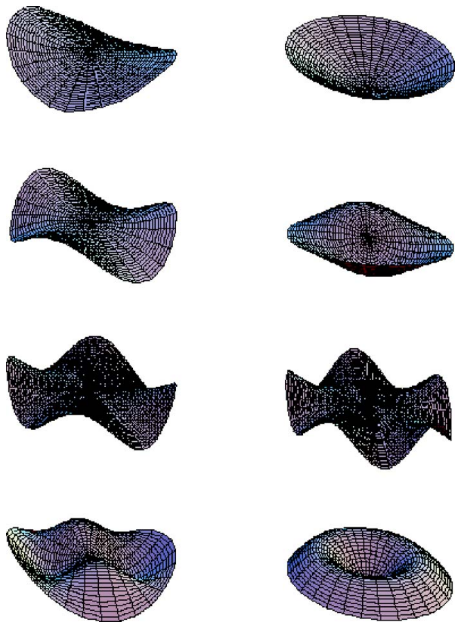

Fig. 7 First eight mode shapes of the circular plate obtained by the proposed method ($N=16$)

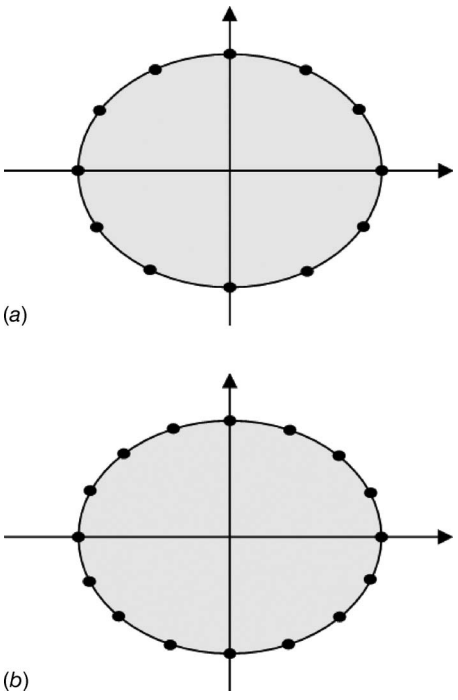

Fig. 8 Discrete boundary nodes of the elliptic plate when (*a*) $N=12$ and (*b*) $N=16$

of the proposed method are summarized in Fig. 3. Note that $\det(\mathbf{SM}_{\text{plate}})$ is divided by $\det(\mathbf{SM}_{\text{mem}})$ to remove the spurious eigenvalues generated due to the incompleteness of the general solution, and that the incompleteness results from choosing only two bases [4,29]. For a more rigorous way of removing the spurious eigenvalues, refer to Chen's paper [31].

On the other hand, $|\mathbf{r}_i-\mathbf{r}_k|$ in Eqs. (21)–(24) should be expressed with the local polar coordinates r_i and θ_i to differentiate $J_0(\Lambda|\mathbf{r}_i-\mathbf{r}_k|)$ and $I_0(\Lambda|\mathbf{r}_i-\mathbf{r}_k|)$ with respect to r_i and θ_i. As illustrated in Fig. 4, $|\mathbf{r}_i-\mathbf{r}_k|$, the distance between nodes P_i and P_k, may be expressed as

$$|\mathbf{r}_i-\mathbf{r}_k| = \sqrt{(x_i-x_k)^2+(y_i-y_k)^2} \tag{25}$$

where (x_i,y_i) and (x_k,y_k) are coordinates of nodes P_i and P_k, respectively, about the global coordinates system (x,y). If using the local polar coordinates r_i and θ_i, (x_i,y_i) can be expressed as

$$(x_i,y_i) = (x_{0i}+r_i\cos\theta_i, y_{0i}+r_i\sin\theta_i) \tag{26}$$

where (x_{0i},y_{0i}) denotes coordinates of origin O_i about the global coordinates system. Finally, substituting Eq. (26) into Eq. (25) yields

$$|\mathbf{r}_i-\mathbf{r}_k| = \sqrt{(r_i\cos\theta_i+x_{0i}-x_k)^2+(r_i\cos\theta_i+y_{0i}-y_k)^2} \tag{27}$$

where x_{0i}, x_k, y_{0i}, and y_k are given by the shape of the plate of interest.

2.5 Divergence Problem. One may notice that Eqs. (21)–(24) cannot be evaluated for $i=k$ because $|\mathbf{r}_i-\mathbf{r}_k|$ is involved in denominators of terms generated when the equations are expanded by applying $L_{M(i)}$ and $L_{V(i)}$ to $J_0(\Lambda|\mathbf{r}_i-\mathbf{r}_k|)$ and $I_0(\Lambda|\mathbf{r}_i-\mathbf{r}_k|)$ (i.e., Eqs. (21)–(24) diverge for $i=k$ because the denominators become zeros). Thus, limit forms of Eqs. (21)–(24) for $i=k$ will be found by approaching node P_k to node P_i as shown in Fig. 4.

From Eq. (26), (x_k,y_k) may also be expressed as

$$(x_k,y_k) = (x_{0i}+r_k\cos\theta_k, y_{0i}+r_k\sin\theta_k) \tag{28}$$

which is substituted into Eq. (27). Equation (27) then leads to

$$|\mathbf{r}_i-\mathbf{r}_k| = \sqrt{r_i^2+r_k^2-2r_ir_k\cos(\theta_k-\theta_i)} \tag{29}$$

from which it may be said that approaching node P_k to node P_i denotes that $r_k\to r_i$ and $\theta_k\to\theta_i$. Thus, the limit values of Eqs. (21)–(24) for $i=k$ are calculated by means of $r_k\to r_i$ and $\theta_k\to\theta_i$ as follows

$$SM_{\text{M}}^{\text{J}}(i,i) = \lim_{\substack{r_k\to r_i\\ \theta_k\to\theta_i}} L_{M(i)}[I_0(\Lambda|\mathbf{r}_i-\mathbf{r}_k|)] = \frac{(1+\nu)}{2}\Lambda^2 \tag{30}$$

$$SM_{\text{M}}^{\text{I}}(i,i) = \lim_{\substack{r_k\to r_i\\ \theta_k\to\theta_i}} L_{M(i)}[I_0(\Lambda|\mathbf{r}_i-\mathbf{r}_k|)] = \frac{(1+\nu)}{2}\Lambda^2 \tag{31}$$

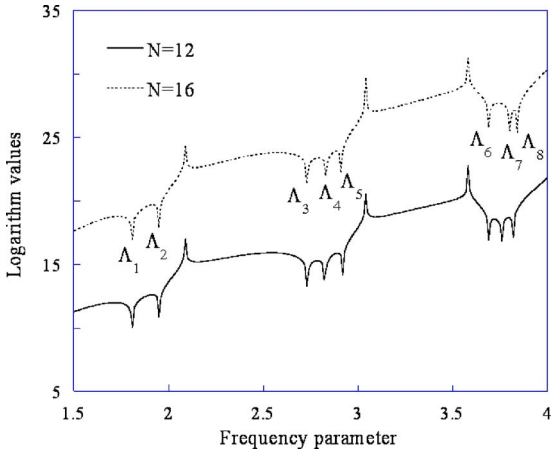

Fig. 9 Logarithm curves for $\det(\mathbf{SM}_{\text{plate}})/\det(\mathbf{SM}_{\text{mem}})$ of the elliptic plate when $N=12$ and $N=16$; the resolution of increment of the frequency parameter is 1/1000

$$SM_{\text{V}}^{\text{J}}(i,i) = \lim_{\substack{r_k\to r_i\\ \theta_k\to\theta_i}} L_{V(i)}[J_0(\Lambda|\mathbf{r}_i-\mathbf{r}_k|)] = 0 \tag{32}$$

$$SM_{\text{V}}^{\text{I}}(i,i) = \lim_{\substack{r_k\to r_i\\ \theta_k\to\theta_i}} L_{V(i)}[I_0(\Lambda|\mathbf{r}_i-\mathbf{r}_k|)] = 0 \tag{33}$$

where $|\mathbf{r}_i-\mathbf{r}_k|$ was given by Eq. (29). For reference, similar work to measure Eqs. (30)–(33) has been done in a previous paper [32].

3 Verification Examples

To verify the proposed method, free vibration analyses of circular, elliptic, and arbitrarily shaped plates with free boundary conditions were carried out. For each case, the eigenvalues obtained by the proposed method were compared with those obtained by another analytical method and FEM (ANSYS). The mode shapes found by the proposed method are also presented in this paper.

3.1 Free Circular Plate. As shown in Fig. 5, the boundary of the free circular plate of unit radius is discretized with 12 and 16 nodes. For reference, the ill-condition of the system matrix occurs for 24 nodes, which is because the distance between adjacent nodes is too close.

Logarithmic values of $\det(\mathbf{SM}_{\text{plate}})/\det(\mathbf{SM}_{\text{mem}})$ for 12 and 16 nodes are plotted as a function of Λ in Fig. 6 where the values of Λ corresponding to the troughs represent the eigenvalues of the plate. In addition, note that the values of Λ corresponding to the peaks in Fig. 6 represent the eigenvalues of the membrane with

Table 2 Eigenvalues of the elliptic plate obtained by the proposed method, Sato's method, and FEM

Eigenvalues	Proposed method		Sato [24]	FEM (ANSYS)		
	$N=12$	$N=16$		4335 nodes	2773 nodes	1778 nodes
Λ_1	1.8058	1.8057	1.806	1.8058	1.8060	1.8065
Λ_2	1.9527	1.9519	None	1.9530	1.9520	1.9523
Λ_3	2.7331	2.7331	2.733	2.7355	2.7344	2.7363
Λ_4	2.8267	2.8307	None	2.8306	2.8308	2.8306
Λ_5	2.9198	2.9119	None	2.9133	2.9117	2.9116
Λ_6	3.6926	3.6929	None	3.6958	3.6937	3.6942
Λ_7	3.7560	3.8032	3.802	3.8016	3.8016	3.8012
Λ_8	3.8174	3.8416	None	3.8400	3.8388	3.8389

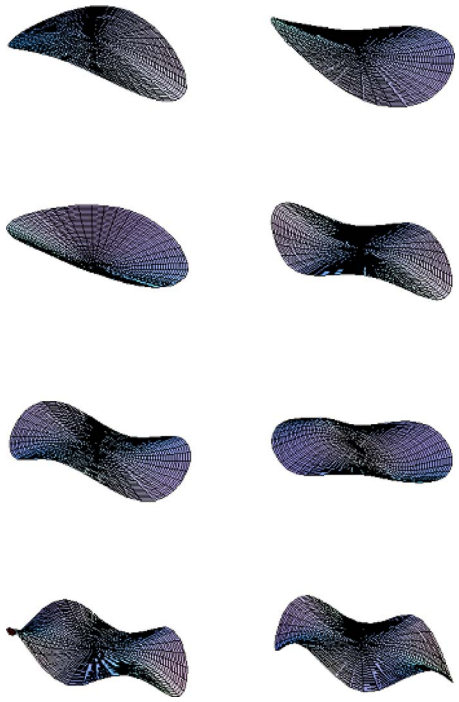

Fig. 10 First eight mode shapes of the elliptic plate obtained by the proposed method ($N=16$)

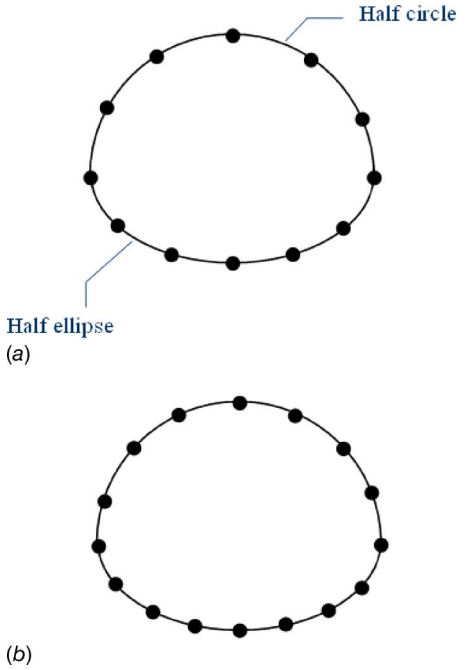

Fig. 11 Discrete boundary nodes of the arbitrarily shaped plate, composed of a half-circle and a half-ellipse, when (*a*) $N=12$ and (*b*) $N=16$

the same shape as the plate. The first eight eigenvalues of the free circular plate obtained by the proposed method, Leissa's source, and FEM (ANSYS) are summarized in Table 1. It may be said that the proposed method yields accurate results for only a small number of nodes, when the eigenvalues by the proposed method for $N=16$ are compared with those by FEM for 4439 nodes. Figure 7 shows the first eight mode shapes of the plate found by the proposed method. The mode shapes were in good agreement with those by FEM, which have been omitted in this paper.

It may be, interestingly, seen in Table 1 that the sixth eigenvalue (Λ_6) was not found for $N=12$. This results from the fact that the sixth mode has too many nodal lines in the circumferential direction to describe the mode shapes with only 12 nodes. On the other hand, although the seventh and eighth modes are higher modes than the sixth mode, they were successfully found for $N=12$. This is because, as shown in Figs. 7(*g*) and 7(*h*), they have small numbers of nodal lines in the circumferential direction, compared with the sixth mode.

In summary, the minimum number of nodes is 16 for the first eight eigenvalues and the maximum number of nodes is 20 for avoiding the ill-condition of the system matrix when the number of nodes is increased by 4. Thus, it may be said that the present method has a proper region in the number of nodes for accurate eigenvalues.

3.2 Free Elliptic Plate. Another verification example is an elliptic plate whose minor axis is unit length and the ratio of the major axis to the minor axis is 1:4. For $N=12$ and $N=16$, the locations of boundary nodes of the plate are illustrated in Fig. 8. In Fig. 9, logarithmic values of $\det(\mathbf{SM}_{\text{plate}})/\det(\mathbf{SM}_{\text{mem}})$ are shown as a function of Λ for the two cases of discretized models (for reference, the ill-condition of the system matrix occurs for 24 nodes). It may be seen in Table 2 that the proposed method yields accurate results that show little difference with FEM results for 4335 nodes. In addition, Fig. 10 shows mode shapes found by the proposed method and they have been checked to agree well with those by FEM (ANSYS).

On the other hand, in Table 2 eigenvalues have also been presented by Sato's method [24], which is by now unique as an analytical method for free vibrations of free elliptic plates to the authors' best knowledge. It should be noticed that Sato's method gives only three eigenvalues among eight ones ($\Lambda_1-\Lambda_8$), but the proposed method successfully gives entire eigenvalues.

3.3 Free Plate of Arbitrary Shape. Finally, free vibration analysis is carried out for an arbitrarily shaped plate for which there exists no analytical solution. As illustrated in Fig. 11, the plate is composed of the half-circle and half-ellipse, of which the minor axis is unit length and the ratio of the major axis to the minor axis is 1:4. In addition, the boundary of the plate is discretized with 12 and 16 nodes.

In Fig. 12, the logarithmic values of $\det(\mathbf{SM}_{\text{plate}})/\det(\mathbf{SM}_{\text{mem}})$ are shown as a function of Λ for $N=8$, $N=12$, and $N=16$ (for reference, the ill-condition of the system matrix occurs for 24 nodes). A comparison between the proposed and the numerical

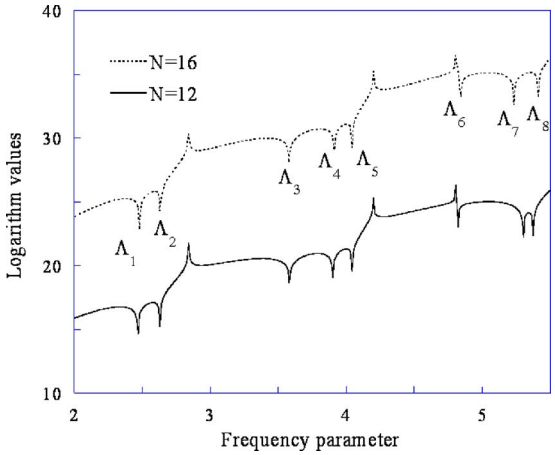

Fig. 12 Logarithm curves for $\det(\mathbf{SM}_{\text{plate}})/\det(\mathbf{SM}_{\text{mem}})$ of the arbitrarily shaped plate when $N=12$ and $N=16$; the resolution of increment of the frequency parameter is 1/1000

Table 3 Eigenvalues of the arbitrarily shaped plate obtained by the proposed method and FEM

Eigenvalues	Proposed method		FEM (ANSYS)			
	$N=8$	$N=12$	$N=16$	4095 nodes	2757 nodes	1513 nodes
Λ_1	2.4230	2.4656	2.4785	2.5078	2.5077	2.5143
Λ_2	2.5653	2.6277	2.6349	2.6379	2.6388	2.6403
Λ_3	3.5737	3.5812	3.5792	3.5601	3.5617	3.5617
Λ_4	None	3.8972	3.9076	3.9202	3.9204	3.9225
Λ_5	None	4.0425	4.0425	4.0449	4.0454	4.0500
Λ_6	4.9431	4.8216	4.8421	4.8309	4.8322	4.8364
Λ_7	None	5.2968	5.2297	5.2233	5.2240	5.2246
Λ_8	5.4725	5.3728	5.4074	5.3995	5.4004	5.4050

method (ANSYS) is summarized in Table 3. It can be found from Table 3 that, although the proposed method uses only a small number of nodes (16 nodes), it gives results close to FEM results computed by using a large number of nodes (4095 nodes). The mode shapes of the plate that were obtained by the present method are shown in Fig. 13, which were found to agree well with those by FEM.

In addition, it may be confirmed from Table 3 that the convergence of eigenvalues is non-monotonic for the third, sixth, and eighth eigenvalues. Thus, it may be concluded that the convergence of the method is non-monotonic. For reference, the non-monotonic convergence of eigenvalues was confirmed in the author's previous papers [4,5].

4 Conclusions

In this paper, the NDIF method has been successfully extended to the free vibration analysis of arbitrarily shaped plates with the free boundary condition. Verification examples show that the proposed method yields accurate eigenvalues and mode shapes extremely close to those from other analytical methods and FEM (ANSYS), even when only a small number of nodes is used compared with FEM. Since the proposed method has been especially developed for plates with only smoothly varying boundaries (note that, due to this specialty, it gives very accurate results), it cannot be applied immediately to plates with straight edges. Thus, a new approach effective for polygonal plates such as triangular and rectangular plates will be presented in another paper following this paper.

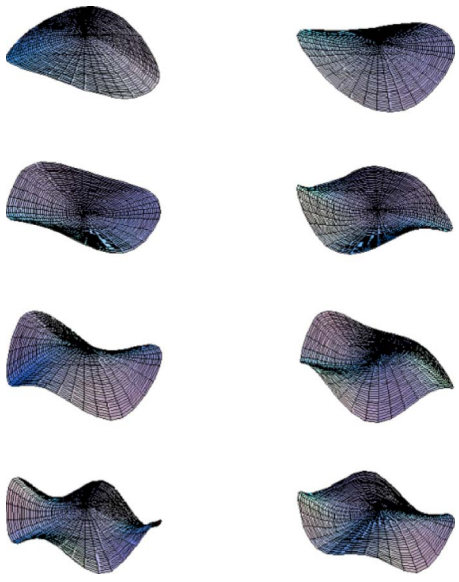

Fig. 13 First eight mode shapes of the arbitrarily shaped plate obtained by the proposed method ($N=16$)

Acknowledgment

This research was financially supported by Hansung University in 2007.

References

[1] Kang, S. W., Lee, J. M., and Kang, Y. J., 1999, "Vibration Analysis of Arbitrarily Shaped Membranes Using Non-dimensional Dynamic Influence Function." J. Sound Vib., **221**, pp. 117–132.

[2] Kang, S. W., and Lee, J. M., 2000, "Eigenmode Analysis of Arbitrarily Shaped Two-dimensional Cavities by the Method of Point-Matching." J. Acoust. Soc. Am., **107**(3), pp. 1153–1160.

[3] Kang, S. W., and Lee, J. M., 2000, "Application of Free Vibration Analysis of Membranes Using the Non-dimensional Dynamic Influence Function." J. Sound Vib., **234**(3), pp. 455–470.

[4] Kang, S. W., and Lee, J. M., 2002, "Free Vibration Analysis of Arbitrarily Shaped Plates With Clamped Edges Using Wave-type Functions." J. Sound Vib., **242**(1), pp. 9–26.

[5] Kang, S. W., 2002, "Free Vibration Analysis of Arbitrarily Shaped Plates With a Mixed Boundary Condition Using Non-dimensional Dynamic Influence Functions." J. Sound Vib., **256**(3), pp. 533–549.

[6] Hughes, T. J. R., 1987, *The Finite Element Method*, Prentice-Hall, Englewood Cliffs, NJ.

[7] Brebbia, C. A., 1978, *The Boundary Element Method for Engineers*, John Wiley & Sons, New York.

[8] Brebbia, C. A., Telles, J. C. F., and Wrobel, L. C., 1984, *Boundary Element Techniques*, Springer-Verlag, New York.

[9] Conway, H. D., 1961, "The Bending, Buckling, and Flexural Vibration of Simply Supported Polygonal Plates by Point-Matching." ASME J. Appl. Mech. **28**, pp. 288–291.

[10] Singh, B., and Chakraverty, S., 1992, "Transverse Vibration of Simply Supported Elliptical and Circular Plates Using Boundary Characteristic Orthogonal Polynomials in Two Variables." J. Sound Vib., **152**(1), pp. 149–155.

[11] Conway, H. D., and Karnham, K. A., 1965, "The Free Flexural Vibration of Triangular, Rhombic and Parallelogram Plates and Some Anologies." Int. J. Mech. Sci., **7**, pp. 811–816.

[12] Mazumdar, J., 1973, "Transverse Vibration of Membranes of Arbitrary Shape by the Method of Constant-Deflection Contours." J. Sound Vib., **27**, pp. 47–57.

[13] Nagaya, K., 1978, "Vibrations and Dynamic Response of Membranes With Arbitrary Shape." ASME J. Appl. Mech., **45**, pp. 153–158.

[14] Durvasula, S., 1969, "Free Vibration of Simply Supported Parallelogrammic Plates." J. Aircr., **6**, pp. 66–68.

[15] Chopra, I., and Durvasula, S., 1972, "Vibration of Simply Supported Trapezoidal Plates, I. Symmetric Trapezoids." J. Sound Vib., **19**, pp. 379–392.

[16] Chopra, I., and Durvasula, S., 1972, "Vibration of Simply Supported Trapezoidal Plates, II. Unsymmetric Trapezoids." J. Sound Vib., **20**, pp. 125–134.

[17] Durvasula, S., 1968, "Natural Frequencies and Modes of Skew Membranes." J. Acoust. Soc. Am., **44**, pp. 1636–1646.

[18] Durvasula, S., 1969, "Natural Frequencies and Modes of Clamped Skew Plates." AIAA J., **7**, pp. 1164–1167.

[19] Hasegawa, M., 1957, "Vibration of Clamped Parallelogrammic Isotropic Flat Plates." J. Aeronaut. Sci., **24**, pp. 145–146.

[20] Hamada, M., 1959, "Compressive or Shear Buckling Load and Fundamental Frequency of a Rhomboidal Plate with All Edges Clamped." Bull. JSME, **2**, pp. 520–526.

[21] Nair, P. S., and Durvasula, S., 1973, "Vibration of Skew Plates." J. Sound Vib., **26**, pp. 1–19.

[22] Dickinson, S. M., 1978, "The Buckling and Frequency of Flexural Vibration of Rectangular, Isotropic and Orthotropic Plates Using Rayleigh's Method." J. Sound Vib., **61**, pp. 1–8.

[23] Leissa, A. W., 1973, "The Free Vibration of Rectangular Plates." J. Sound

Vib., **31**, pp. 257–293.
[24] Sato, K., 1973, "Free-Flexural Vibrations of an Elliptical Plate With Free Edges." J. Acoust. Soc. Am., **54**, pp. 547–550.
[25] Zhang, X., Song, K. Z., Lu, M. W., and Liu, X., 2000, "Meshless Methods Based on Collocation With Radial Basis Functions." Comput. Mech., **26**, pp. 333–343.
[26] Alves, C. J. S., and Antunes, P. R. S., 2005, "The Method of Fundamental Solutions Applied to the Calculation of Eigenfrequencies and Eigenmodes of 2D Simply Connected Shapes." Comput., Mater., Continua, **2**(4), pp. 251–265.
[27] Chen, J. T., Chen, I. L., and Lee, Y. T., 2005, "Eigensolutions of Multiply-Connected Membranes Using Method of Fundamental Solution, Engineering Analysis With Boundary Elements." Eng. Anal. Boundary Elem., **29**(2), pp. 166–174.
[28] Reutskiy, S. Y., 2005, "The Method of Fundamental Solutions for Eigenproblems With Laplace and Biharmonic Operators." Comput., Mater., Continua, **2**(3), pp. 177–188.
[29] Chen, J. T., Lee, Y. T., Chen, I. L., and Chen, K. H., 2004, "Mathematical Analysis and Treatment for the True and Spurious Eigenequations of Circular Plates in the Meshless Method Using Radial Basis Function." J. Chin. Inst. Eng., **27**(4), pp. 547–561.
[30] Meirovitch, L., 1967, *Analytical Methods in Vibrations*, Macmillan, New York, pp. 179–189.
[31] Chen, J. T., Chen, I. L., Chen, K. H., and Lee, Y. T., 2003, "Comments on Free Vibration Analysis of Arbitrarily Shaped Plates With Clamped Edges Using Wave-type Functions." J. Sound Vib., **262**(2), pp. 370-378.
[32] Chen, J. T., Chang, M. H., Chen, K. H., and Lin, S. R., 2002, "The Boundary Collocation Method With Meshless Concept for Acoustic Eigenanalysis of Two-dimensional Cavities Using Radial Basis Function." J. Sound Vib., **257**(4), pp. 667–711.